Fabrication of GaAs-based photonic band gap materials

W. D. Zhou,[a] P. Bhattacharya, J. Sabarinathan, and D. H. Zhu
Solid State Electronics Laboratory, Department of Electrical Engineering and Computer Science, University of Michigan, Ann Arbor, Michigan 48109-2122

(Received 10 October 1999; accepted 28 December 1999)

A relatively simple technique for fabrication of GaAs-based quasi-three-dimensional photonic crystals has been investigated. Selective impurity-induced layer disordering and wet oxidation techniques are utilized. Fourier-transform infrared spectroscopy measurement reveals a stop band between 15 and 20 μm for a sample with scattering center spacing of 6.3 μm. Another narrow transmittance dip is observable in the wavelength range of 1.1–1.58 μm, with an attenuation of 12 dB at 1.18 μm. The process is reproducible and lends itself to integration with other optoelectronic and electronic devices on the same substrate. © *2000 American Vacuum Society.*
[S0734-211X(00)04803-4]

I. INTRODUCTION

The development of photonic band gap (PBG) materials [or photonic crystals (PC)] has been fueled by the possibility of understanding and realizing new physical phenoma such as photonic band gaps, light localization, single mode light emission, lossless light guiding, and enhanced nonlinearities.[1,2] Such PBG materials are of great interest owing to the possibility of spontaneous emission control. Inhibited spontaneous emission could lead to thresholdless lasers or single mode light emitting diodes (LEDs), which may lower the power requirements and increase the efficiency and reliability. Enhanced spontaneous emission, on the other hand, would allow faster modulation speeds for optical interconnects. By tuning the photonic band gap to overlap with the electronic band edge, electron-hole recombination can be controlled in a photonic band gap crystal, leading to enhanced efficiency and reduced noise in the operation of various optoelectronic devices, such as low-loss resonators, optical transistors, bandpass filters, and photonic integrated circuit (PIC), etc. By introducing ''photonic defects'' into the regular lattice of a photonic crystal, a localized state may be generated within the forbidden gap[2–4] which can essentially be a tiny optical cavity and perhaps the core of a photonic band gap disk laser.[5]

Unlike semiconductor crystals, photonic crystals need to be created artificially. One of the biggest challenges is to create three-dimensional (3D) III–V semiconductor based PBG materials operating at optical wavelength. It is desirable to create 3D crystals with complete 3D photonic band gap based on direct semiconductors, such as GaAs. InP, etc. in which the radiative efficiency is high. Since the spacing of the dielectric scatterers should be of the order of λ/n in these materials, where λ is the vacuum wavelength and n is the refractive index of the material, submicron pattern technique is needed in order to fabricate PBG materials operating at optical wavelength. Finally, for some of the applications described above, it may be desirable to delineate waveguides on which contacts can be formed. Above all, the processing technique should be relatively simple and reproducible.

Many approaches have been investigated to fabricate the photonic crystals, such as mechanically drilling air channels, chemically etching holes, e-beam patterned dry etching techniques and wafer bonding techniques, etc.[6–9] Success in producing one-, two-, and three-dimensional photonic band gaps for microwave and millimeter-wave radiation, and for shorter optical wavelengths in one- and two-dimensional structures has been reported. Recently, photonic gaps have been demonstrated in nanometer scale ''woodpile'' structures.[10–12]

The GaAs-based processing technique that we will describe here is a standard microelectronic fabrication technology by utilizing the traditional Zn diffusion technique and AlGaAs wet oxidation technique. Without etching or drilling air channels, which are the most dominant approaches in making current PBG crystals, the diffraction loss associated with the semiconductor–air interface is reduced significantly in this all-semiconductor structure. Light localization was verified by transmission experiment on different lengths of waveguide. Defects in our PBG crystals are created during the process, since our process incorporates the random nature of zinc diffusion induced disordering. Fourier-transform infrared spectroscopy (FTIR) and transmission experiments were performed in the fabricated PBG materials.

II. FABRICATION

The PBG crystal fabrication started with a single molecular beam epitaxial (MBE) grown heterostructure, shown in Fig. 1(a). After growing a 0.1 μm GaAs buffer layer, a 0.2 μm $Al_{0.98}Ga_{0.02}As$ etch stop layer, and a 0.5 μm GaAs etch protection layer, the active region is grown. It consists of a 1-μm-thick layer of $Al_{0.98}Ga_{0.02}As$ followed by six periods of 0.18 μm of $Al_{0.8}Ga_{0.2}As$ and a multiquantum-well (MQW) region. The latter consists of 20 pairs of 20 Å GaAs and 150 Å $Al_{0.8}Ga_{0.2}As$ layers. The total thickness of the active region is 3.14 μm. A protective 200 Å GaAs cap layer is finally grown. The entire structure is undoped.

The process steps to form the photonic crystal are outlined in Fig. 2. The key steps are a Zn-diffusion induced

[a]Electronic mail: wzhou@umich.edu

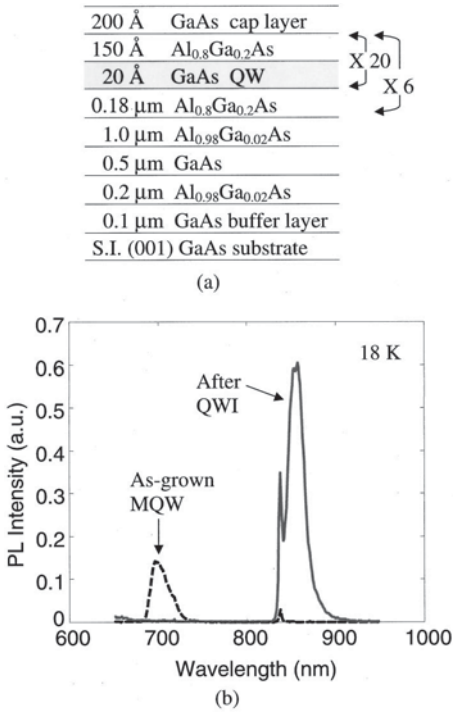

FIG. 1. (a) GaAs-based heterostructure grown by molecular beam epitaxy and used to form the photonic bandgap (PBG) crystal; (b) low-temperature (18 K) photoluminescence (PL) spectra of the sample.

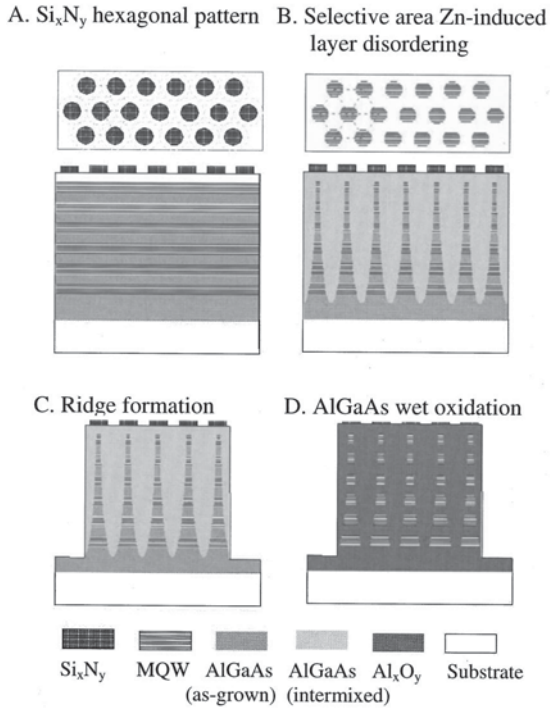

FIG. 2. Process steps used to form PBG crystal. The key steps are the IILD of the MQW regions with zinc and the wet oxidation of AlGaAs regions to form $Al_xO_y(n\sim1.5)$.

quantum well intermixing (QWI) of the MQW regions to form a uniform alloy[13]—known as impurity-induced layer disordering (IILD)—and a wet oxidation[14] of epitaxially grown and intermixed AlGaAs alloy regions to form the stable oxide Al_xO_y with a refractive index of ~1.5. Figure 1(b) shows the low temperature photoluminescence spectrum peak originated from the MQW region in the as-grown sample disappeared after IILD or QWI.

As shown in Fig. 2(a), a hexagonal pattern, acting as the Zn diffusion mask, is formed by lithography and reactive ion etching (RIE) of 0.1 μm plasma enhanced chemical vapor deposition (PECVD) deposited Si_xN_y. The center-to-center spacing a is ~6 μm. The relatively large diameter is chosen to minimize lateral diffusion of zinc. The deep zinc diffusion step is carried out with a $ZnAs_2$ source in an evacuated quartz ampoule at 575 °C for 90 min. IILD takes place selectively in the MQW regions through the openings between the Si_xN_y disks and converts it into a uniform $Al_{0.71}Ga_{0.29}As$ alloy, left with different sizes of high index small MQW cylinders, as shown in Fig. 2(b). Ridges of width 35 μm are formed by standard optical lithography and a combination of RIE and H_3PO_4 wet etching, as shown in Fig. 2(c). The etching is done down to the 0.5 μm GaAs layer. The sample is then inserted in an open-tube quartz furnace and lateral wet oxidation is performed at 450 °C for 15 h by flowing N_2 saturated with water vapor by bubbling it through a water bath held at 95 °C. It is worthwhile to note that the relatively long oxidation time selected is due to the relatively low oxidation temperature chosen in order to minimize the Zn redistribution in the crystal. Both epitaxially grown $Al_{0.8}Ga_{0.2}As$ and intermixed $Al_{0.71}Ga_{0.29}As$ regions are uniformly oxidized to form the insulator Al_xO_y, as demonstrated in Fig. 2(d). It may be noted that under the hydrolysis conditions used, the thin 150 Å $Al_{0.8}Ga_{0.2}As$ layers within the nonintermixed MQW regions are not oxidized.[15] We have now created a photonic crystal in which small MQW regions of average refractive index ~3.55 are embedded in an Al_xO_y medium of refractive index ~1.5. The scanning electron microscope (SEM) image of the waveguide along with a schematic are shown in Fig. 3.

A disadvantage of this process is the considerable lateral diffusion of zinc during the deep diffusion step. It is estimated that the scattering center radius r varies in the range of 0.15–1.5 μm. Because of such considerable lateral diffusion of Zn with depth, an asymmetric structure is created, which could result in lower injection efficiency and certain randomness. We therefore choose to describe our structure as a quasi-3D, weakly disordered, crystal.

The photonic crystal is cleaved with different waveguide lengths ranging from 0.6 to 1.8 mm and the substrate is removed by using lapping and the selective wet etching techniques, including a combination of NH_4OH and HF solution for selective etching of GaAs and AlGaAs layers. A black wax protection layer on top and SiO_2 antireflection (AR) coating on the waveguide facets are used prior to substrate etching in order to protect the photonic crystal and the waveguide cleaved facets. The final PBG waveguide is placed on a silica glass substrate for waveguide transmission experiment to avoid mode leakage into GaAs substrate.

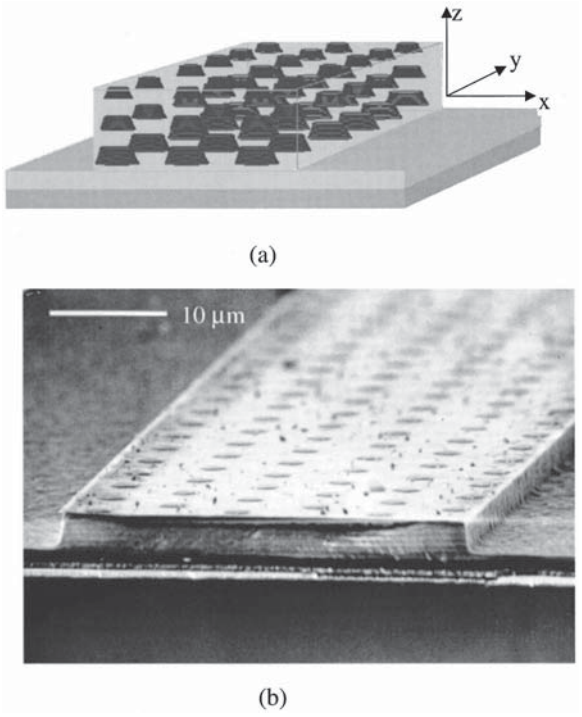

FIG. 3. (a) Schematic and (b) scanning electron microscope (SEM) image of fabricated GaAs-based PBG waveguide. The MQW scattering regions are faintly visible in the SEM image. Si_xN_y disks (reduced in size during processing) are seen on the top surface.

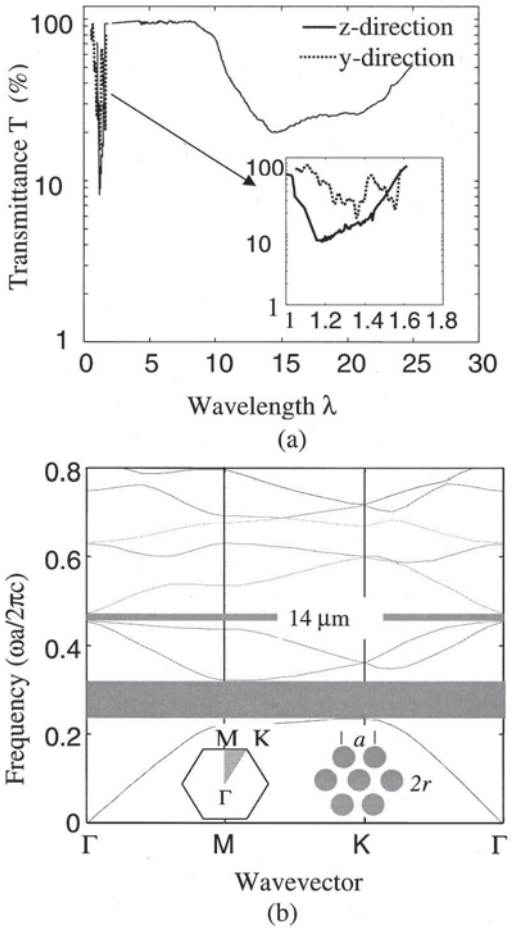

FIG. 4. (a) Transmission spectra shows a stop band centered at 14.8 μm along the z direction for a PBG material with $a=6.3$ μm. Also shown are the stop bands around 1 μm measured along the y and z directions; (b) calculated band structure based on expansion theory with $n_l=1.5$, $n_h=3.5$, $r=1.5$ μm, $a=6.3$ μm; note a gap centered at 14 μm.

III. EXPERIMENTAL RESULTS

Surface normal (z direction) FTIR was performed at room temperature, in the wavelength range of 2.5–25 μm on samples in which the GaAs substrate was thinned down to 100 μm and polished. Since the beam size (~5 mm) is much larger than the waveguide width, samples with several parallel waveguides were used. The measured spectrum is shown in Fig. 4(a). The spectrum is normalized by the measured spectra of the GaAs substrate and Al_xO_y of thicknesses identical to those in the photonic crystals. A transmittance dip between 15 and 20 μm is observed, which fits reasonably well with the results[16] of a 2D crystal scaled from the microwave measurements, with the parameters of our structure. As shown in Fig. 4(b), our calculation has revealed a gap around 14 μm for an ideal 2D PBG structure with parameters same as our fabricated quasi-3D structure. Transmission spectroscopies on both surface normal (z direction) and waveguide (y) direction were also done in the wavelength range of 0.9–1.6 μm with a photomultiplier or a Ge detector. Again, the measured data was normalized with respect to GaAs and Al_xO_y. The measured spectra are also shown in Fig. 4(a), with a 12 dB attenuation at 1.18 μm along the z direction. A transmission peak is also noted within the stop band in the y direction. The exact origin of the second gap at the lower wavelength is not fully understood, but its presence is confirmed with measurement in two orthogonal directions. Similar gaps have been theoretically calculated by Maystre *et al.* in photonic crystals composed of dielectric rods in air or air holes in dielectric medium[17] and have been attributed to grating effects due to Wood's anomalies. It may be a pseudogap caused by a randomness or weak disorder due to the uncontrolled Zn diffusion process. In the crystal reported here, the perfect periodicity is destroyed by process-induced nonuniformity of the scatterer size. These aspects are under investigation.

The transmission coefficient, T, as a function of waveguide length, has been measured in our fabricated PBG waveguide in order to investigate possible light localization due to the nonuniformity induced randomness. The GaAs substrates were completely removed in these samples, in order to eliminate mode leakage into substrates. The cleaved facets of waveguides, varying in length from 0.6 to 1.8 mm, were end fired with TE polarized light from a 1.15 μm He–Ne laser and the guided (transmitted) power at the output was measured with a power meter. We did not observe any evidence of light leaking into the thin Al_xO_y supporting layer underneath. The measured data is shown in Fig. 5(a). A distinct exponential decay of the transmission with waveguide length is observed and assuming that the decay is $\sim\exp(-L/L_{\mathrm{loc}})$, where L_{loc} is the localization length. We have also fitted the same data with a T-L^{-2} dependence in

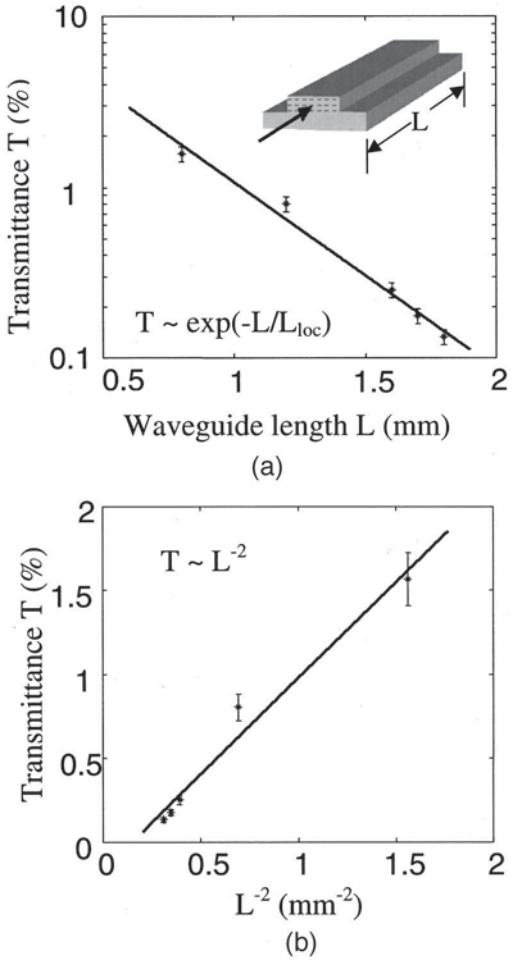

FIG. 5. Measured transmission of end-fired 1.15 μm light through waveguides as a function of guide length. The polarization of the incident light is parallel to the heterostructure layers. The measured transmission is fitted to (a) exponential and (b) quadratic variation with waveguide length. Both fits are good, indicating photon localization.

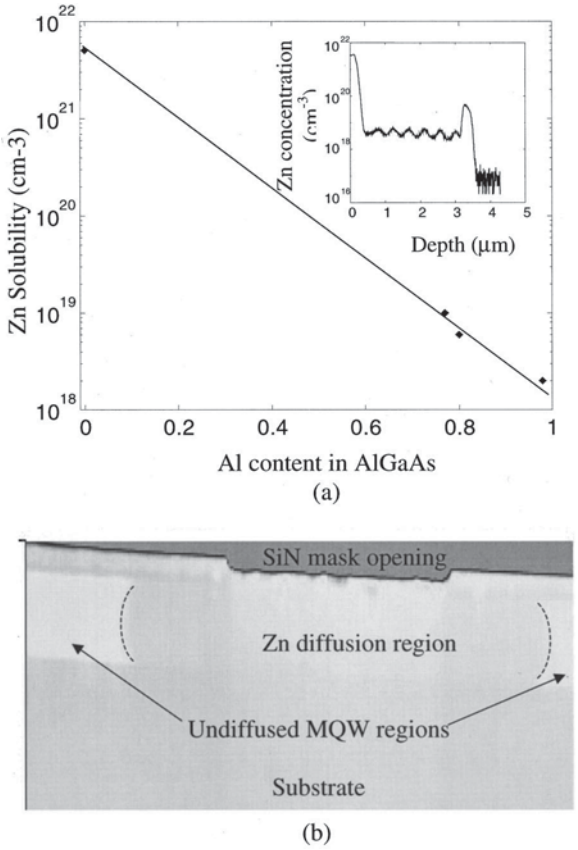

FIG. 6. (a) Zn solubility vs aluminum content x in $Al_xGa_{1-x}As$ based on SIMS results, with inset showing the SIMS profile of Zn concentration along depth in the structure after IILD; (b) scanning capacitance measurement result showing the Zn lateral spreading along depth for a simple GaAs/AlGaAs MQW structure.

accordance with the scaling theory of localization at the localization transition.[3,4,18] The fit is shown in Fig. 5(b). For a T-L^{-2} dependence, an average transport velocity $\nu = 3.81 \times 10^7$ cm/s is estimated, assuming an average mean free path of 1.73 μm. The phase velocity for this device, derived from a geometrical optics estimation with a fill factor of 0.2, is about 1.54×10^{10} cm/s. Therefore, it can be said with some caution that light localization occurs in our samples, possibly due to the localized defect states, observed in the transmission experiments.

IV. DISCUSSION

A high Al content of both epitaxial grown $Al_xGa_{1-x}As$ barrier region and the intermixed $Al_xGa_{1-x}As$ is desirable for a high oxidation rate and short oxidation time. The oxidation rate of $Al_xGa_{1-x}As$ decreases dramatically with decreasing the Al content.[19] On the other hand, in order to effectively disorder the quantum well region through Zn induced disordering, a high Zn concentration in the order of $10^{19}\,cm^{-3}$ or above is required.[20] While SIMS results show that the Zn solubility N_{Zn} in the $Al_xGa_{1-x}As$ alloy is strongly dependent on the Al content x, as shown in Fig. 6(a), N_{Zn} decreases exponentially with increasing x. To satisfy the $N_{Zn} > 10^{19}\,cm^{-3}$ requirement for disordering, the aluminum content in $Al_xGa_{1-x}As$ must be less than 0.8. An optimized aluminum content x must be selected. Our final design uses $x = 0.8$ for epitaxially grown $Al_xGa_{1-x}As$ and $x = 0.71$ for intermixed $Al_xGa_{1-x}As$.

The relatively simple process described here is very reliable compared to other techniques and compatible to the standard microfabrication process. The only disadvantage of the process is the considerable lateral diffusion of Zn during the deep diffusion step. We have determined that the lateral spread almost matches the depth for 1.4 μm diffusion from scanning capacitance measurement, as shown in Fig. 6(b). However, this provides the randomness in the size and spacing of the MQW scatterers and helps us to realize a disordered photonic crystal. It is estimated that the size of the scattering centers varies in the range of 0.3–3 μm. By using a well-controlled process, such as ion-implantation induced disordering or impurity-free vacancy disordering techniques, to minimize the lateral spreading, the spacing can be further decreased.

V. CONCLUSION

We demonstrate here a processing technique with which we have created a quasi-three-dimensional photonic crystal. A stop band around 1.5 μm has been obtained both experimentally and theoretically. The technique is versatile and reproducible work is in progress to improve the size uniformity and scale down the scatterer spacing by using electron-beam lithography and better controlled disordering techniques.

ACKNOWLEDGMENT

The work was partially supported by the Army Research Office.

[1]E. Yablonovitch, J. Opt. Soc. Am. B **10**, 283 (1993).
[2]S. John, Phys. Rev. Lett. **58**, 2486 (1987).
[3]D. Wiersma, P. Bartolini, A. Lagendijk, and R. Righini, Nature (London) **390**, 671 (1997).
[4]J. D. Joannopoulos, P. Villeneuve, and S. Fan, Nature (London) **386**, 143 (1997).
[5]R. K. Lee, O. J. Painter, B. Kitzke, A. Scherer, and A. Yariv, Electron. Lett. **35** (1999).
[6]K. Ho, C. Chan, C. Soukoulis, R. Biswas, and M. Sigalas, Solid State Commun. **89**, 413 (1994).
[7]C. C. Cheng, V. Arbet-Engels, A. Scherer, and E. Yablonovitch, Phys. Scr., T **68**, 17 (1996).
[8]E. Özbay, E. Michel, G. Tuttle, R. Biswas, M. Sigalas, and K. Ho, Appl. Phys. Lett. **64**, 2059 (1994).
[9]V. Berger, O. Gauthier-Lafaye, and E. Costard, Electron. Lett. **33**, 425 (1997).
[10]S. Y. Lin *et al.*, Nature (London) **394**, 251 (1998).
[11]S. Noda, N. Yamamoto, and A. Sasaki, Jpn. J. Appl. Phys., Part 2 **36**, L909 (1996).
[12]S. Kawakami, in the 6th International Workshop on Femosecond Technology, TB-11, Makuhari Messe, Chiba, Japan, 1999 (unpublished).
[13]W. Laidig *et al.*, Appl. Phys. Lett. **38**, 776 (1981).
[14]J. M. Dallesasse, N. Holonyak, Jr., S. R. Sugg, T. A. Richard, and N. El-Zein, Appl. Phys. Lett. **57**, 2844 (1990).
[15]J.-H. Kim, D. Lim, K. Kim, G. Yang, K. Lim, and H. Lee, Appl. Phys. Lett. **69**, 3357 (1996).
[16]P. Bhattacharya, W. D. Zhou, D. H. Zhu, and J. Sabarinathan, Appl. Phys. Lett. **75**, 1670 (1999).
[17]D. Maystre, Pure Appl. Opt. **3**, 975 (1994).
[18]Z. Genack and N. Garcia, J. Opt. Soc. Am. B **10**, 408 (1993).
[19]K. D. Choquette *et al.*, IEEE J. Quantum Electron. 916 (1997).
[20]D. G. Deppe and N. Holonyak, Jr., J. Appl. Phys. **64**, R93 (1988).